Effect of geometrical parameters towards the heat transfer in modified 80kW DC motor with radial water cooling duct.

Pongsatit Isarankura Na Ayuthaya[1], Jarruwat Charoensuk[1,*] and Chadchai Srisurangkul[2]

[1]Department of Mechanical Engineering, Faculty of Engineering, King Mongkut's Institute of Technology Ladkrabang, Bangkok, Thailand 10520

[2]National Metal and Materials Technology Center, Pathumthani, Thailand 12120

[*]Corresponding Author: kcjarruw@kmitl.ac.th, Tel: 0-2329-8351, Fax: 0-2329-8352

Abstract

One of the risks in using 80 kW DC induction motor as a prime mover for high performance vehicles is thermal failure due to cumulative heat generation from electrical loss. This unwanted heat could be taken out of the unit by a water coolant. This work deals with the effect of geometrical parameters on heat removal capability of the unit. The case of study can be divided into three parts. Part one is on the effect of cooling duct size. Part two is on the effect of base diameter and part three is on the number of cooling ducts. The model which has the best result among others is the 7.5 millimeter duct size with one cooling duct in the model of 30 centimeter of base diameter.

Keywords*:* DC Motor, Cooling, Three-dimensional, CFX, Heat transfer

1. Introduction

"In the future, the number of vehicles will grow up. If these vehicles are propelled by internal combustion engines, where will the oil come from?"[1]. This is a big question for the industrial community which is heavily dependent on energy. Moreover, global warming has become a social issue; the environmental protection and energy consumption are the most popular topics for those who are concerned about the earth. At that point many researchers try to look for technologies which are cleaner and more efficient than conventional ones.

The technologies of future vehicles are developed in many countries from many companies. There are many components that must be developed, especially the driving system, which focus on how to increase the efficiency.

The performances of an electric vehicle are usually shown in terms of acceleration performance and energy consumption. The acceleration performances are starting acceleration, passing ability and maximum speed. In an electrical vehicle, only electric motor delivers torque to the driven wheels. Thus the vehicle performance is completely determined by the torque speed or power-speed characteristic of the electric motor. In order to achieve these requirements, it needs to improve the motor characteristic especially energy consumption [2].

It is well known that the DC motor is not a perfect energy conversion device. It also generates four major losses which are (1) heat generation by ball bearings, (2) heat generation by the electric motor in rotor and stator “Fig. 1”, (3) heat generation due to viscosity shear of air by the rotating components of the spindle, and (4) qualitative description of power distribution from spindle heat sources to heat sinks [3]. These heat losses will increase the energy consumption and it also cause damages directly to the induction wire of the motor. At that point the heat loss can be damaging to the motor. These heat losses must be removed from the motor.

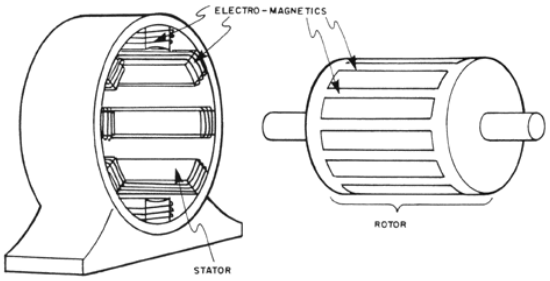

Fig. 1 The stator and rotor of electric motor

2. Problem Specification

2.1 Problem

One of the risks in using 80 kW DC induction motor as a prime mover for high performance vehicles is thermal failure due to cumulative heat generation from electrical loss. This unwanted heat could be taken out of the unit by a water coolant.

2.2. Investigation

Aim of this research is to study an effect of temperature distribution and pressure drop which depend on geometry of the motor housing. This research can be divided into three parts. Part one concerns about the effect of cooling duct size. Part two is on the effect of base diameter and part three is the number of cooling ducts.

2.2. Assumption

According to EU regulation (IE2: High efficiency), the motor must have minimum efficiency of 95%. For safety reason, this study has adopted heat loss at 10% or 8 kW instead of 5% [4].

3. Mathematical Models

The energy conservation in the system is determined using the energy balance equation (Eq.1).

$$E_{in} - E_{out} = \Delta E_{system} \quad (1)$$

Heat flux generated by heat loss is determined by equation (2), when $\dot{Q}_{loss}$ is determined by equation (3).

$$q" = \frac{\dot{Q}_{loss}}{A} \quad (2)$$

$$\eta_{th} = \frac{\dot{W}_{net}}{\dot{E}_{in}} = \frac{\dot{W}_{net}}{\dot{W}_{net}+\dot{Q}_{loss}} \quad (3)$$

Equation (4) of thermal energy is used for calculation of total heat rejection of cooling water.

$$\dot{Q} = \dot{m}_c c_{pc}(T_{c,out} - T_{c,in}) \quad (4)$$

Equation (5) is used for explaining the simple phenomena of heat resistance and temperature distribution of motor housing next to cooling duct at base diameter described in section (5.1.2) [5].

$$\dot{Q} = (2\pi L)\frac{T_1 - T_2}{\ln(r_2/r_1)} \quad (5)$$

Equation (6) is used for explaining the simple phenomena of pressure drop which is described in section (5.2) **[6].**

$$\Delta P = \overline{\gamma} h_L \quad (6)$$

$$h_L = h_{L\,major} + h_{L\,minor} \quad (6a)$$

$$h_{L\,major} = f\frac{l}{D}\frac{v^2}{2g} \quad (6b)$$

$$h_{L\,minor} = K_L\frac{v^2}{2g} \quad (6c)$$

4. Research methodology

4.1. Case study

The study on effects of (1) duct sizing, (2) base diameter and (3) number of ducts in 20 millimeters of ring width are described as follow.

4.1.1 Cooling duct size

The red box on the cross-section view of cooling duct as seen in “Fig. 2b” shows sizing of cooling duct which have five mm of height and “x” mm of width. In this case study, the “x” value varies from 5, 7.5, 10, 12.5, 15 to 17.5 mm.

4.1.2 Cooling duct location

This case focuses on the effect of base diameter in terms of temperature distribution when the black line in “Fig. 2a” is the base diameter of the cooling duct. In this case, 7.5 mm. width and 5 mm. height of duct size is used and base diameter is varied from 30, 32 to 34 cm.

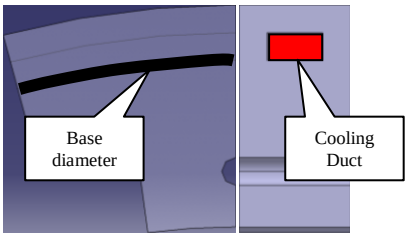

(a) (b)

Fig. 2a Front view of cooling duct (15 mm.).

Fig. 2b Cross-section view of cooling duct.

4.1.3 Number of cooling duct per ring

In section 4.1.1 and 4.1.2 only base diameter and duct size are varied but the number of cooling ducts remains the same as one cooling duct. In this case, the effect of the number of cooling ducts is studied by using 1-duct model compare with 2-duct model. Both models contain 5 mm width of cooling duct size and 20 mm of ring width “Fig. 3”.

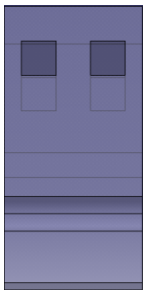

Fig. 3 Cross-section at 2 cooling duct model

4.2. Computation procedure

The study on effective parameter in terms of temperature distribution in each case requires a commercial program code name “CFX ANSYS 12” as a tool for analysis.

By using the CFX program, a domain of solid and fluid must be set up. Steel is used as a solid domain and water at 25℃ is used as a fluid domain. For boundary condition, it can be divided into three zones, first zone is heat source (1), second is symmetry (2) and the last one is adiabatic wall zones “Fig. 4”

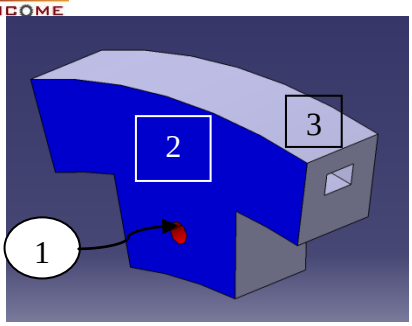

Fig. 4 Zones of boundary condition

By assuming the heat source was generated in the middle of the teeth, Zone 1 in "Fig. 4" shows a heat source which is set up in the program as a heat flux wall, when the value of heat flux is 212,210 W/m^2 or 66.67 W per heat source zone.

In terms of fluid domain, the boundary condition of cooling water flow is to have inlet at pole no.12 and outlet at pole no.6 as seen in "Fig. 5". The flow rate and temperate at inlet port are 0.1 kg/s and 60℃ and the pattern of flow is turbulent and the reason is shown in table 1.

Table 1 the flow pattern in each cooling duct size.

Size (mm)	Velocity (m/s)	Reynolds number	Flow Pattern
5.0	2.00	2.11E+04	Turbulent
7.5	1.33	1.69E+04	Turbulent
10.0	1.00	1.41E+04	Turbulent
12.5	0.80	1.20E+04	Turbulent
15.0	0.67	1.05E+04	Turbulent
17.5	0.57	9.37E+03	Turbulent

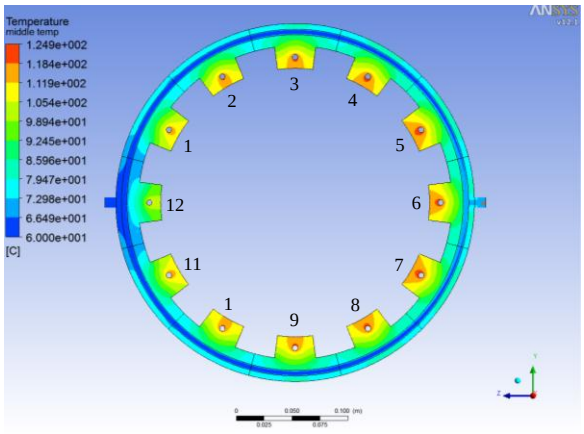

Fig. 5 The located of the pole.

5. Result and Discussion

5.1. Results

5.1.1. Cooling duct size

In a 5-mm cooling duct size model, it was found that the temperature was 60℃ at the entrance of inlet port and the temperature rose to 61.88℃ when it flowed out of channel. The profile of temperature distribution is shown in "Fig. 6".

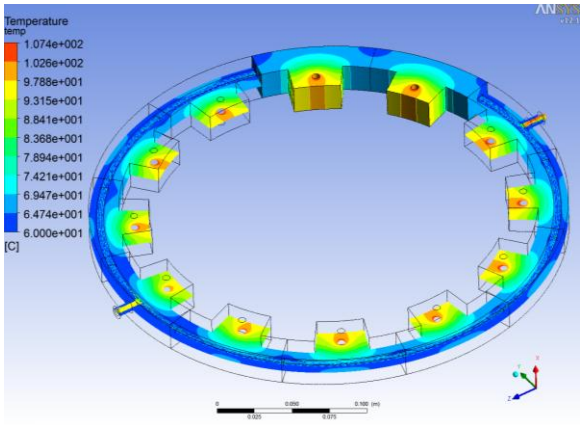

Fig. 6 Temperature distribute in the middle of cooling duct (5mm.)

From "Fig. 6" the highest temperature are pole no.5 and pole no.7. At this point "Fig. 7" the temperature is 94.41℃.

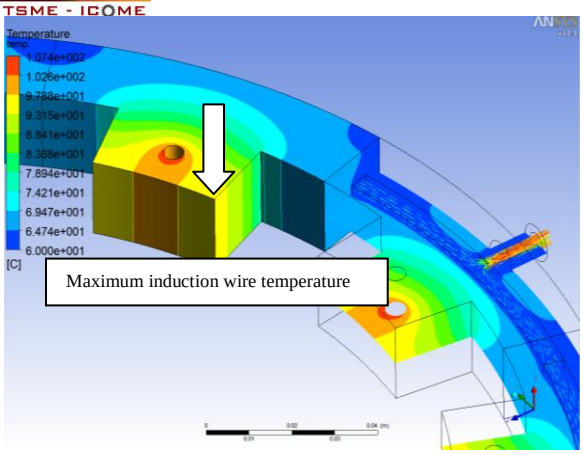

Fig. 7 Temperature distribute in pole no.5 (5mm.)

At the cross-section of the cooling duct "Fig. 8", it was found that the changes of temperature profile between cooling duct wall and ring boundary had a low temperature region located at the cooling duct wall and the temperature increased to its peak at ring boundary.

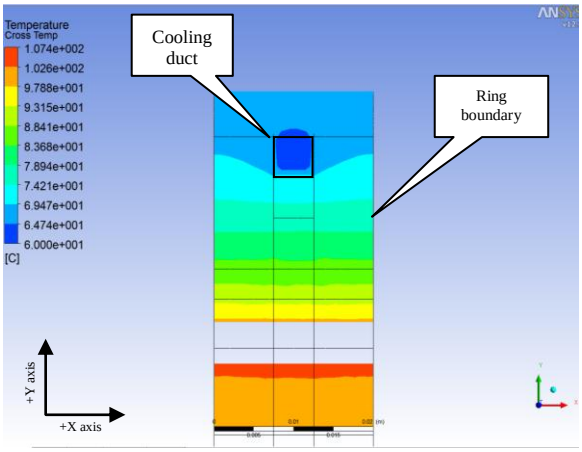

Fig. 8 Temperature distribute in the cooling duct cross-section.

The temperature profile is the same for the other models with small differences. Table 2 shows a result in details.

5.1.2. Cooling duct base diameter

In this part, the profiles of temperature distribution are similar to 7.5-mm cooling duct size model studied in section 5.1.1. But the pole no.5 and no.7 of 30-cm, 32-cm and 34-cm base diameter of cooling duct have 95.11, 101.65 and 108.79 respectively. The result of this part can be explained in Table 3 and the profile of temperature in 34-cm base diameter of cooling duct which has a maximum temperature at pole no.5 and pole no.7 is shown in "Fig. 9".

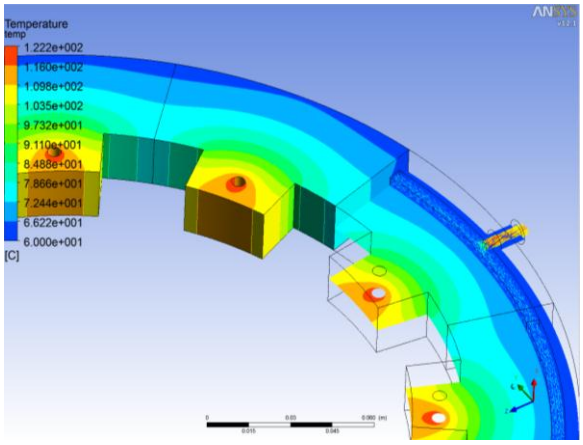

Fig. 9 Temperature distribute at pole no.5 (34cm.)

According to "Eq. (5)", if the base diameter is increased from 30 cm to 32 cm or 34 cm, the heat flow resistance will be increased too.

Table2 the simulation results in term of cooling duct sizing at 0.1kg/s of cooling water mass flow rate.

Descriptions	Duct size (mm.)					
	5.0	7.5	10.0	12.5	15.0	17.5
Pressure drop (kPa.)	23.63	22.29	23.43	23.54	24.03	23.68
Maximum temperature at pole no.5 and no.7 (C.)	94.41	95.12	95.65	96.42	97.34	99.21
Outlet coolant temperature (C.)	61.88	61.89	61.89	61.87	61.87	61.88
Heat reject (W.)	0.786	0.790	0.790	0.782	0.782	0.786

Table 3 the simulation results in term of base diameter at 0.1kg/s of cooling water mass flow rate.

Descriptions	Base diameter (cm.)		
	30	32	34
Pressure drop (kPa.)	22.29	21.77	22.00
Maximum temperature at pole no.5 and no.7 (C.)	95.11	101.65	108.79
Outlet coolant temperature (C.)	61.89	61.9	61.9
Heat reject (W.)	0.79	0.794	0.794

5.1.3. Number of cooling duct per ring

The result of 1-cooling-duct model and 2-cooling-duct model provides a significant difference because in 2-cooling-duct model the distance between ducts is shorter than 1-duct model by half. The temperature distributions in cross-section for both models are shown in “Fig. 10” and “Fig. 11”. The result of this case can be explained in Table 4.

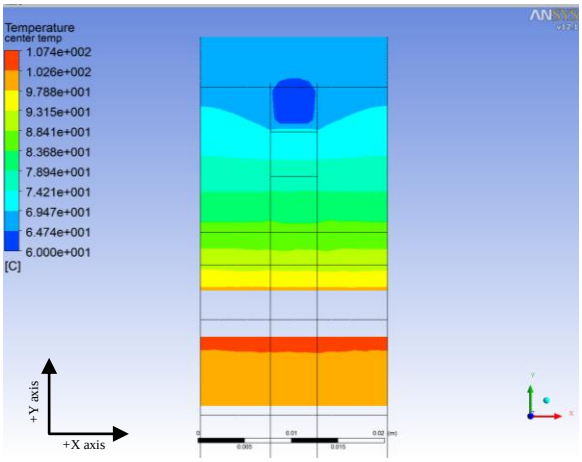

Fig. 10 Cross-section temperature distribution of one duct model.

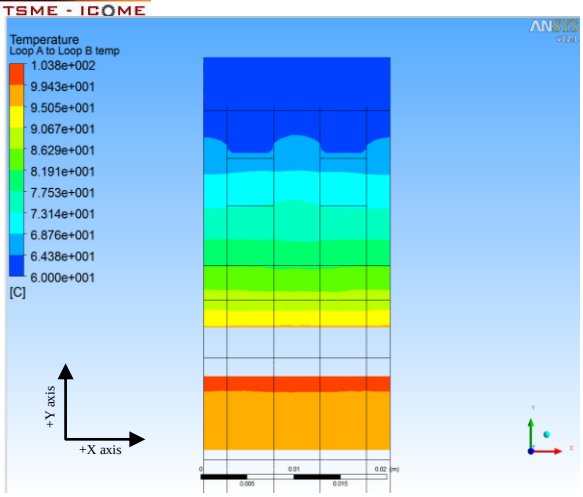

Fig. 11 Cross-section temperature distribution of two duct model.

Table 4 the simulation results in term of number of cooling duct at 0.1kg/s of cooling water mass flow rate.

Descriptions	Number of cooling duct	
	1	2
Pressure drop (kPa.)	22.29	21.77
Maximum temperature at pole no.5 and no.7 (C.)	95.11	101.65
Outlet coolant temperature (C.)	-273.15	-273.15
Heat reject (W.)	0.79	0.794

5.2 Discussion

According to the results in section "5.1.", many data show the advantages and disadvantages in each case study (section "5.1.1.", "5.1.2." and "5.1.3."). In section "5.1.1.", according to "Eq. (6) - (6c)" The temperature deferential of cooling water between inlet temperature and outlet temperature are small. Therefore, the effect of density due to the temperature is negligible and the pressure is decreased when duct size is increased but in Table 1 the pressure drop in each duct size does not vary in linear function with size of channel flow due to domination of minor loss. In this case, there are 2 types of pressure drop. First is major loss and the other is minor loss. For a major loss the main factor is the size but the difference is small. It can be assumed that this major loss provides only small influences. For a minor loss, it relates to an increase in area (pole no.12), a decrease in area (pole no.6), 3-way and Bending in circle. The minor loss will be increased, if the size of duct is increased. It will be convenient if the area of inlet port can be adjustable for decreasing pressure drop in these areas. For a maximum temperature at pole no.5 and pole no.7, it was found that when the duct size is increased the temperature will be increased too, because velocity of water will decrease. It can be concluded that temperature is strongly related to water speed.

In section "5.1.2.", the maximum temperature at pole no.5 and pole no.7 in table 3 increases if the base diameter is increased, its relationship can be explained in "eq. (5)".

When compare between "Fig. 10" and "Fig.11" in section "5.1.3.", the profiles of temperature are not the same. In "Fig. 11" low temperature zone is larger than that in "Fig. 10" because it is easier to control a temperature around cooling duct wall in model of 2 cooling ducts. When considering about temperature distribution in cross-section the temperature will be increased along thickness of ring ("+X" and "-X" axis), so that if the model has many cooling ducts, it is easy to control a temperature profile at the middle of both ducts in condition of multi-cooling ducts model.

6. Conclusion

In this study, it can be concluded for 5 mm of inlet port of 7.5 mm with one cooling duct in 30 cm of base diameter gives the best result for this research.

7. Acknowledgement

Special thanks to National Metal and Materials Technology Center.

8. References

8.1 Article in Journals

[1] C.C. Chan, K.T. Chau, “Modern electric vehicle technology”, *engineering philosophy of EV development*, pp. 1.

[2] M. Ehsani, Y. Gao, and S. Gay, “Characterization of Electric Motor Drives for Traction Applications”, *IEEE paper, ISBN: 0-7803-7906-3 This paper appears in: Industrial Electronics Society*, Vol.1, pp.891, 2003.

[3] C.H. Huang, H.C. Lo, “A three-dimensional inverse problem in estimating the internal heat flux of housing for high speed motors”, *Applied Thermal Engineering* 26 (2006) 1515–1529

8.2 Books

[4] James Larminie, John Lowry, “Electric Vehicle Technology Explained”, ISBN 0-470-85163-5, pp.176

[5] Yunus A. Çengel, “Heat Transfer: A Practical Approach”, 2nd edition, pp. 46, 49, 679.

[6] Bruce R. Munson, Donald F. Young, Theodore H. Okiishi, “Fundamentals of Fluid Mechanics”, 5th edition, ISBN-10: 0-471-72578-1, pp. 430, 432, 437.